
A real-time motion planning scheme for collaborative robots using HRI-based cost function

Khawaja Fahad Iqbal*

System Robotics Laboratory,
Department of Robotics,
Tohoku University,
Sendai, Japan
Email: fahad@irs.mech.tohoku.ac.jp

and

RISE Laboratory,
Department of Robotics and Artificial Intelligence,
School of Mechanical and Manufacturing Engineering (SMME),
National University of Sciences and Technology (NUST),
Islamabad, Pakistan

*Corresponding author

Akira Kanazawa

System Robotics Laboratory,
Department of Robotics,
Tohoku University,
Sendai, Japan
Email: kanazawa@irs.mech.tohoku.ac.jp

Silvia Romana Ottaviani

Leonardo Company,
Via Giovanni Agusta 520, 21017 Cascina Costa,
VA, Italy
Email: silvia.r.ottaviani@gmail.com

Jun Kinugawa and Kazuhiro Kosuge

System Robotics Laboratory,
Department of Robotics,
Tohoku University,
Sendai, Japan
Email: kinugawa@irs.mech.tohoku.ac.jp
Email: kosuge@tohoku.ac.jp

Abstract: In this paper, we propose a novel scheme for real-time motion planning of a collaborative robot that assists its fellow human worker in performing assembly tasks by delivering parts and tools to the worker. In the proposed scheme, the delivery position of the parts and tools is determined first, based on a cost function relating to the safety, visibility, and arm comfort terms of the worker by solving the non-convex optimisation problem in real-time using a random sampling-based algorithm in the vicinity of the worker's current position. Then, model predictive control (MPC)-based trajectory planner directly generates a collision-free robot trajectory from the current robot configuration to the delivery configuration under velocity and acceleration constraints of the robot. The proposed motion planning scheme is implemented in the actual collaborative robot system and the effectiveness of the proposed scheme is illustrated experimentally.

Keywords: collaborative robot; motion planning; human-robot interaction.

Reference to this paper should be made as follows: Iqbal, K.F., Kanazawa, A., Ottaviani, S.R., Kinugawa, J. and Kosuge, K. (2021) 'A real-time motion planning scheme for collaborative robots using HRI-based cost function', *Int. J. Mechatronics and Automation*, Vol. 8, No. 1, pp.42–52.

Biographical notes: Khawaja Fahad Iqbal received his MS in Biongingering and Robotics from the Tohoku University, Sendai, Japan in 2017.

Akira Kanazawa received his MS in Bioengineering and Robotics from the Tohoku University, Sendai, Japan, in 2017.

Silvia Romana Ottaviani received her BE in Electronics Engineering and MS in Control Engineering both from the La Sapienza University, Rome, Italy in 2017.

Jun Kinugawa is an Assistant Professor in the Department of Robotics, Tohoku University. He received his PhD in Bioengineering and Robotics from the Tohoku University, Sendai, Japan, in 2011.

Kazuhiro Kosuge is a Professor in the Department of Robotics at Tohoku University, Japan. He received his BS, MS and PhD in Control Engineering from the Tokyo Institute of Technology, in 1978, 1980, and 1988 respectively. From 1982 through 1990, he was a research associate in the Department of Control Engineering at the Tokyo Institute of Technology. From 1990 to 1995, he was an Associate Professor at the Nagoya University. From 1995, he has been at Tohoku University. He is IEEE Fellow, JSME Fellow, SICE Fellow, RSJ Fellow and a JSAE Fellow. He was the President of IEEE Robotics and Automation Society for 2010–2011 and IEEE Division X Director for 2015–2016. He is a member of IEEE-Eta Kappa Nu and the IEEE Vice President for Technical Activities for 2020.

1 Introduction

Collaborative robots are used in the industry to assist human workers and improve their productivity in performing tasks that cannot be automated easily using industrial robots. ISO 10218-1 (2011) and ISO 10218-2 (2011) standards were issued for making the use of robots in human environments possible without isolating the robots from human workers by amending the original ISO standard 10128. The amendment of the ISO standard has enabled system integrators to build more flexible and efficient systems assuming collaboration of the human workers and the robots. Today, major robot manufacturers are producing their own collaborative robots, and these robots are being used in many industries.

A collaborative robot system, PaDY (in-time parts/tools delivery to the robot) has been developed to reduce the load of the human worker and improve productivity by delivering parts and tools to the worker in the automobile assembly processes in Kinugawa et al. (2010). The efficiency of the delivery task has been further improved by the predictions of the worker's movements in Tanaka et al. (2012). The prediction-based concept has been enhanced by developing a new motion planning system which calculates the motion trajectory taking the uncertainty of prediction into account in Kanazawa et al. (2019).

This system allows the robot to deliver parts and tools without unnecessary waiting time at the delivery position while avoiding contact with workers moving around in the workspace. However, the human worker cannot always repeat the same motion. Since the delivery position is determined heuristically based on the pre-planned work schedule of the human worker in Tanaka et al. (2012) and Kanazawa et al. (2019), therefore the optimal delivery position may be different from the heuristically determined position. This could prevent the worker from smoothly carrying out the task after receiving the parts and tools from the robot. To further improve the efficiency of the

collaborative work, the robot needs to deliver the parts and tools to an optimal position for the worker.

Several studies have addressed the issue relating to the optimal delivery position from the human robot interaction (HRI) perspective. Mainprice et al. (2011) proposed the path planner to reach the delivery position selected based on the cost map using constraints such as visibility, safety and arm comfort by solving a cost function using a random sampling method.

This concept was applied to the robot-human handover problem. Vahrenkamp et al. (2016) determined the handover position to reduce the path length and energy consumption in an interaction workspace of a robot and a human. Aleotti et al. (2014) presented a novel system for robot-human handover that maximised user's convenience defined by the orientation of the object. Cakmak et al. (2011) proposed the method to decide the delivery position based on user's preference. These methods work well in a static environment where the delivery position does not vary for the robot.

Under the assumption that the human could not repeat the same movement, the trajectory needs to be planned for the observed human motion in real-time. This trajectory planning can be done by solving a nonlinear optimisation problem defined by a cost function related to HRI as a function of the human motion. The random sampling-based path planning used in Mainprice et al. (2011) and Vahrenkamp et al. (2016) solves a nonlinear optimisation problem defined by the cost function related to HRI and has been applied to actual collaborative systems such as Li and Shah (2019) and Wei and Ren (2018). However, the trajectory of the robot along the planned path needs to be generated to control a robot.

Several local optimisation planners such as Ratliff et al. (2009) and Schulman et al. (2013), and global optimisation planners such as Kim and Lee (2015) and Andersson et al. (2016) have been proposed to compute trajectories directly by solving optimisation problems. The

local optimisation planners struggle to effectively solve the nonlinear optimisation including HRI-based costs. The global optimisation planners are computationally too expensive to have a solution in real-time.

In this paper, we propose an alternative real-time motion planning scheme considering the HRI-based cost function. The contributions of this paper are summarised as follows:

- 1 Estimation of an optimal delivery position is formulated as a non-convex optimisation problem with a cost function defined by analytical representation of HRI constraints.
- 2 A real-time robot trajectory planning scheme is proposed by combining a sampling-based local search method for the non-convex optimisation problem and an MPC-based direct trajectory planning method.
- 3 The proposed method plans a collision-free trajectory under robot velocity and acceleration constraints.
- 4 Experimental results illustrate that the proposed system can be applied to real delivery tasks in an automotive assembly process.

The rest of the paper is organised as follows. Section 2 provides the architecture and the details of the proposed motion planning system. Section 3 describes the experimental results. Section 4 concludes the research.

2 Proposed motion planning scheme

The system architecture of the proposed scheme is shown in Figure 1. The scheme consists of two parts, i.e., delivery position determination, and trajectory planning. The delivery position determination part calculates a feasible delivery position based on the human body skeleton data obtained from the sensor. The robot trajectory planning part calculates the trajectory from the current configuration to the goal configuration which is given from the delivery position determination part. A model predictive control (MPC) scheme is used to plan the robot trajectory. The robot is controlled along the trajectory by a robot motion controller.

2.1 Delivery position determination

Human body skeleton data obtained from the sensor is used to calculate the HRI cost function relating to visibility, safety, and arm comfort. The concept of the HRI cost function has been previously proposed in studies such as Mainprice et al. (2011) and Vahrenkamp et al. (2016). We redefine HRI-related cost function based on the target scenario.

In the following part of this paper, the sensor coordinate frame and the human body orientation are defined in a planer workspace as shown in Figure 2 for the simplicity of the discussions.

2.1.1 Visibility cost

The visibility cost function is defined to keep the delivery position within the visual range of the human worker. The concept of the visibility cost has been proposed by Sisbot et al. (2007a) for planners of mobile robots. We assume that the human gazes at the robot without rotating his/her head and define the cost function as a function of the body orientation.

To calculate the visibility cost of the worker, the system needs to derive the body orientation. Let θ_{body} be the body orientation of the worker in the sensor coordinate Σ_{Sensor} . As shown in Figure 2, θ_{body} is defined from the worker's left shoulder position $\mathbf{p}_{lsh} = (x_{lsh}, y_{lsh})$ and the right shoulder position $\mathbf{p}_{rsh} = (x_{rsh}, y_{rsh})$ as

$$\theta_{body} = -\tan^{-1} \left(\frac{x_{lsh} - x_{rsh}}{y_{lsh} - y_{rsh}} \right) \quad (1)$$

Using this body orientation θ_{body} , the visibility cost C_V for the delivery position $\mathbf{p}_{del} = (x_{del}, y_{del})$ is calculated as follows:

$$C_V = \frac{1}{2} k_v * (\Delta\theta_{del-body})^2 \quad (2)$$

$$\Delta\theta_{del-body} = -\tan^{-1} \left(\frac{x_{del} - x_{body}}{y_{del} - y_{body}} \right) - \theta_{body} \quad (3)$$

where $\mathbf{p}_{body} = (x_{body}, y_{body})$ is the centroid of the worker's body and k_v is a weighting factor. An example of the visibility cost function is shown in Figure 3 where red circles indicate the positions of human shoulders.

2.1.2 Safety cost

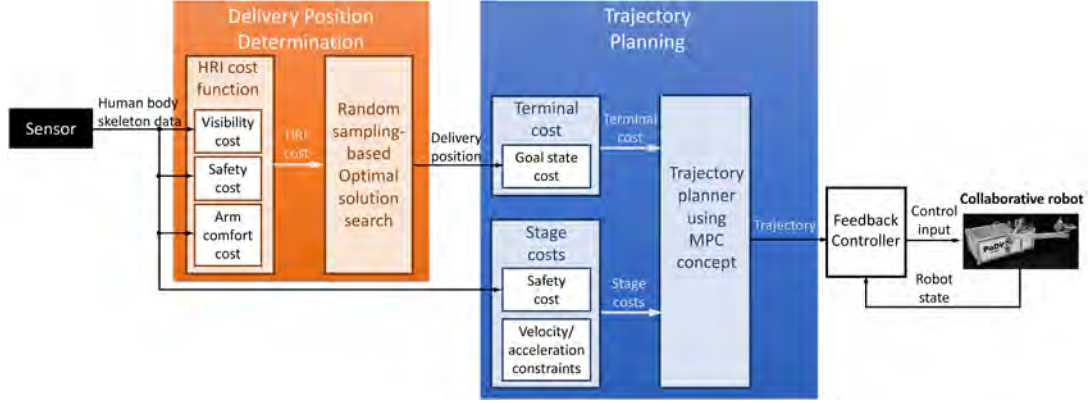
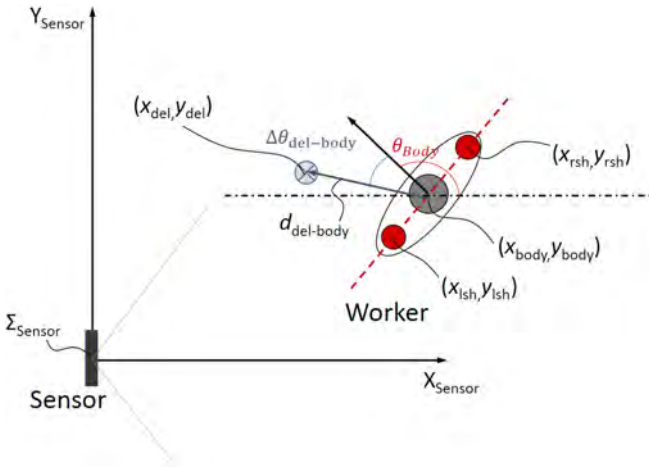
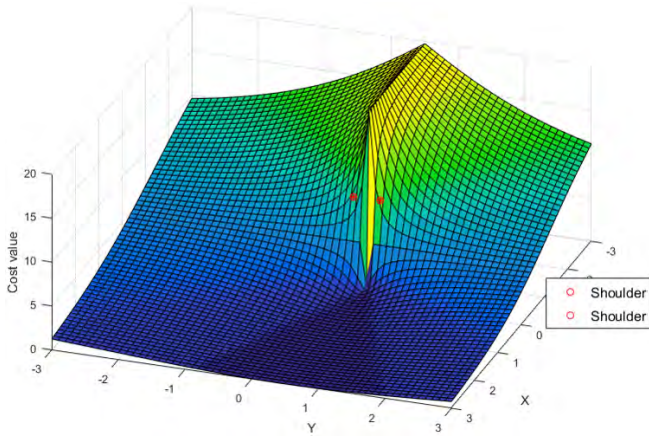
The safety cost is defined as a function of the distance between the delivery position and the centroid of the worker's body. This function prevents the robot from colliding with the worker. To ensure collision avoidance even for the moving worker, the safety cost function is defined using an artificial potential field proposed by Khatib (1985). The safety cost is expressed as follows:

$$C_S = \begin{cases} 0 & \text{if } d_{del-body} \geq d_{max} \\ k_s * \left(\frac{1}{\|d_{del-body}\|} - \frac{1}{d_{max}} \right)^2 & \text{otherwise} \end{cases} \quad (4)$$

where $d_{del-body}$ is the distance between the delivery position \mathbf{p}_{del} and the centroid of the human body \mathbf{p}_{body} . The cost function C_S is zero when the $d_{del-body}$ is equal to or larger than d_{max} , otherwise it becomes positive when the $d_{del-body}$ is smaller than d_{max} . An example of the visibility cost function is shown in Figure 4.

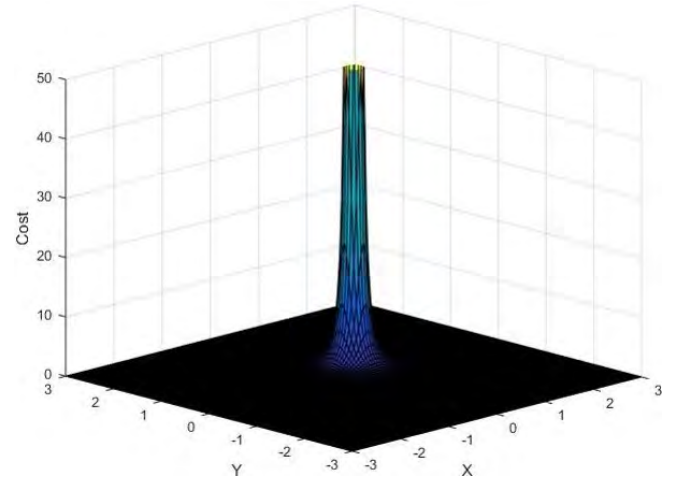
2.1.3 Arm comfort cost

This cost takes into account the worker's arm length and posture to determine the comfortable distance of the delivery position from the centroid of the human body. The concept was first introduced by Sisbot et al. (2007b) and was then refined by Mainprice et al. (2011).

Figure 1 System configuration of our proposed scheme (see online version for colours)

Figure 2 Definition of human body orientation in planer workspace (see online version for colours)

Figure 3 Visibility cost (see online version for colours)


We define the arm comfort as a function of joint angles of the human arm. The arm posture is estimated using human skeleton data obtained by the sensor. Although the human arm is considered as 4 degrees of freedom (3 in the shoulder, 1 at the elbow), the arm posture is estimated assuming the elbow angle is a constant as written in Kashi et al. (2012). In this paper, the average of the elbow angle observed during reaching motions is used as the constant. In addition, the height of the delivery position is assumed

constant and determined based on the position of the robot's end effector of our experimental system, PaDY, which is a 2 DOF planer manipulator.

Figure 4 Safety cost (see online version for colours)


Using these assumptions and the inverse kinematics, the posture of a human arm \mathbf{h} is calculated as a 4-dimensional vector. The cost function for the arm comfort C_A is the sum of three functions as

$$C_A = C_{A,r} + C_{A,l} \quad (5)$$

$$C_{A,*} = C_{a1,*} + C_{a2,*} + C_{a3,*}, \quad (* = r \text{ or } l) \quad (6)$$

Note that $C_{A,*}$ is calculated for both a right arm and a left arm. The first term $C_{a1,*}$ calculates the distance in the joint space between the current worker's arm posture $\mathbf{h}_{cur,*}$ and its resting posture $\mathbf{h}_{rest,*}$. The first term is expressed as

$$C_{a1,*} = k_{a1} * \sum_{j=1}^N \left(\frac{h_{rest,*j} - h_{cur,*j}}{h_{range,*j}} \right)^2 \quad (7)$$

where k_{a1} is a weighting factor and N is the degrees of freedom of the human arm, that is, $N = 4$, and $h_{range,*j}$ is the movable range of j^{th} joint ($j = 1, \dots, 4$).

The second term $C_{a2,*}$ is designed to keep the delivery position away from the joint limits of the human arm. By considering the mean posture $\mathbf{h}_{mean,*}$ based on both the

upper limit $h_{\max,*}$ and the lower limit $h_{\min,*}$ for each joint of the human arm, the second term is expressed as

$$C_{a2,*} = k_{a2} * \sum_{j=1}^N \left(\frac{h_{\text{mean},*,j} - h_{\text{cur},*,j}}{h_{\text{range},*,j}} \right)^2 \quad (8)$$

where k_{a2} is a weighting factor.

The third term is related to the dominant hand, i.e., whether the worker prefers to use his/her right hand or his/her left hand. Note that the worker may be required to use his/her non-dominant hand because of the kinematic constraints the robot and the delivery point. To reduce the opportunity to use the non-dominant hand, the third term puts a penalty on the delivery position using the non-dominant hand. The third term is represented as follows

$$C_{a3,*} = \begin{cases} 0 & \text{if } * = \text{dominant hand} \\ k_p & \text{if } * = \text{non-dominant hand} \end{cases} \quad (9)$$

where k_p is the penalty for using non-dominant hand.

2.1.4 Calculation of delivery position

The optimal delivery position $\mathbf{p}_{\text{del,opt}}$ is calculated based on the following cost function:

$$\text{Cost}(\mathbf{p}_{\text{del}}) = C_S(\mathbf{p}_{\text{del}}) + C_V(\mathbf{p}_{\text{del}}) + C_A(\mathbf{p}_{\text{del}}) \quad (10)$$

The non-convex optimisation of equation (10) is solved by a random sampling-based approach. We adopt the transition-based rapidly-exploring random tree (TRRT) proposed in Jaillet et al. (2008) to solve this problem to avoid the local minima. Although this method is originally intended for path planning, we only use it to find the optimal solution in the vicinity of the worker. This provides a fast global optimal solution, which is input to the direct trajectory planner as a goal position (see Section B).

The pseudo code for delivery pose determination algorithm is shown in Algorithm 1. First, a random position \mathbf{p}_{rand} is sampled from the sampling area S_{near} which is calculated by $\mathbf{p}_{\text{worker}}$ and r_{sample} . Then, the current solution \mathbf{p}_{cur} is moved by a small value δ in the direction of the sampled position \mathbf{p}_{rand} . Next, a transition test proposed in Jaillet et al. (2008) is performed using the cost of the current solution Cost_{cur} and of the new solution Cost_{new} and the distance $d_{\text{new-cur}}$ between \mathbf{p}_{cur} and \mathbf{p}_{rand} . If the conditions of the transition test are met, the new solution is adopted as the current optimal solution. After repeated calculations, the final calculated solution is adopted as the optimal solution $\mathbf{p}_{\text{del,opt}}$.

Algorithm 1 Delivery position determination using TRRT

Input: Current worker's position $\mathbf{p}_{\text{worker}}$,

Sampling range r_{sample} ,

HRI cost function $\text{Cost}(\mathbf{p}_{\text{del}})$,

Output: Optimal delivery position $\mathbf{p}_{\text{del,opt}}$

- 1: Set the sampling area S_{near} using $\mathbf{p}_{\text{worker}}$ and r_{sample}
- 2: $\mathbf{p}_{\text{cur}} \leftarrow \text{Sample}(S_{\text{near}})$
- 3: $\text{Cost}_{\text{cur}} \leftarrow \text{Cost}(\mathbf{p}_{\text{cur}})$
- 4: $\text{Counter} \leftarrow 0$

- 5: **while** $\text{Counter} \leq \text{Counter}_{\text{max}}$ **do**
- 6: $\mathbf{p}_{\text{rand}} \leftarrow \text{Sample}(S_{\text{near}})$
- 7: $\mathbf{p}_{\text{new}} \leftarrow \mathbf{p}_{\text{cur}} + \delta(\mathbf{p}_{\text{rand}} - \mathbf{p}_{\text{cur}})$
- 8: $\text{Cost}_{\text{new}} \leftarrow \text{Cost}(\mathbf{p}_{\text{new}})$
- 9: **if** $\text{TransitionTest}(\text{Cost}_{\text{new}}, \text{Cost}_{\text{cur}}, d_{\text{new-cur}})$ **then**
- 10: $\mathbf{p}_{\text{cur}} \leftarrow \mathbf{p}_{\text{new}}$
- 11: $\text{Cost}_{\text{cur}} \leftarrow \text{Cost}_{\text{new}}$
- 12: $\text{Counter} \leftarrow 0$
- 13: **else**
- 14: $\text{Counter} \leftarrow \text{Counter} + 1$
- 15: **end if**
- 16: **end while**
- 17: $\mathbf{p}_{\text{del,opt}} \leftarrow \mathbf{p}_{\text{cur}}$
- 18: **return** $\mathbf{p}_{\text{del,opt}}$

2.2 Trajectory planning

As a direct trajectory planner, we adopt the planner based on a receding horizon strategy, MPC. The concept of the receding horizon is widely used in real-time robot applications, such as task-parameterised motion planning in Calinon et al. (2014), haptic assistance in Hernández et al. (2012), physical human-robot interaction in Tonietti et al. (2005), and multi-agent motion planning in Du Toit and Burdick (2012).

The cost function used for MPC consists of a terminal cost and a stage cost. The terminal cost only considers the desired terminal state of the robot. The stage cost considers the state of the robot along with the robot trajectory from the current configuration to the goal configuration. A unique part of the proposed system is that the delivery position determined by minimising the HRI cost function is used for the terminal cost. This strategy generates a trajectory that reaches the delivery position based on the HRI cost in real-time.

The cost function J optimised in the proposed planner is expressed by the following equation:

$$J = \varphi(\mathbf{q}(t + T_o)) + \int_t^{t+T_o} (L_1(\dot{\mathbf{q}}(k)) + L_2(\mathbf{q}(k))) dk \quad (11)$$

where T_o is the trajectory length, $\mathbf{q} = (\boldsymbol{\theta}, \dot{\boldsymbol{\theta}})^T$ is the state vector of the robot, $\boldsymbol{\theta} = (\theta_1, \theta_2, \dots, \theta_{N_j})^T$ is a vector composed of joint angles of the manipulator and N_j is the degrees of freedom of the manipulator. $\varphi(\mathbf{q}(t + T_o))$ is the terminal and is expressed as

$$\varphi(\mathbf{q}(t + T_o)) = \frac{1}{2} (\mathbf{F}\mathbf{K}_{N_j}(\mathbf{q}(t + T_o)) - \mathbf{x}_{\text{del}})^T R (\mathbf{F}\mathbf{K}_{N_j}(\mathbf{q}(t + T_o)) - \mathbf{x}_{\text{del}}) \quad (12)$$

where $\mathbf{F}\mathbf{K}_j = (\mathbf{p}, \mathbf{v})^T$ is the forward kinematics of the robot to convert the robot joint state \mathbf{q} to the j^{th} joint position \mathbf{p}_j and velocity \mathbf{v}_j in the workspace. In particular, $\mathbf{F}\mathbf{K}_{N_j}$ corresponds to the state of the robot's endpoint. $\mathbf{x}_{\text{del}} = (\mathbf{p}_{\text{del,opt}}, \mathbf{0})^T$ is the terminal state based on the calculated optimal delivery position.

The stage costs $L_1(\dot{\mathbf{q}}(k))$, $L_2(\mathbf{q}(k))$ are the stage costs and expressed as

$$L_1(\dot{\mathbf{q}}(k)) = \frac{1}{2} \sum_{j=1}^{N_j} r_j (B_{vel,j}(\dot{\theta}_j(k)) + B_{acc,j}(\ddot{\theta}_j(k))) \quad (13)$$

$$L_2(\mathbf{q}(k)) = w \sum_{j=1}^{N_j} C_S(\mathbf{FK}_{p,j}(\mathbf{q}(k))) \quad (14)$$

$L_1(\dot{\mathbf{q}}(k))$ is the penalty function to ensure that the robot moves under the velocity and acceleration constraints. $B_{vel,j}(\dot{\theta}_j(k))$ and $B_{acc,j}(\ddot{\theta}_j(k))$ are expressed as follows:

$$B_{vel,j}(\dot{\theta}_j(k)) = \begin{cases} 0 & (\|\dot{\theta}_j\| \leq \dot{\theta}_{max,j}) \\ (\|\dot{\theta}_j\| - \dot{\theta}_{max,j})^2 & (\|\dot{\theta}_j\| > \dot{\theta}_{max,j}) \end{cases} \quad (15)$$

$$B_{acc,j}(\ddot{\theta}_j(k)) = \begin{cases} 0 & (\|\ddot{\theta}_j\| \leq \ddot{\theta}_{max,j}) \\ (\|\ddot{\theta}_j\| - \ddot{\theta}_{max,j})^2 & (\|\ddot{\theta}_j\| > \ddot{\theta}_{max,j}) \end{cases} \quad (16)$$

where $\dot{\theta}_{max,j}$ is the maximum angular velocity of the j^{th} joint and $\ddot{\theta}_{max,j}$ is the maximum angular acceleration of the j^{th} joint.

$L_2(\mathbf{q}(k))$ is the artificial potential to avoid the worker. As shown in equation (14), the proposed planner includes the safety cost, equation (4), in the stage costs, because the safety cost has to be considered in the entire robot's operational area. $\mathbf{FK}_{p,j}$ is the forward kinematics of the robot to convert the robot joint angle $\boldsymbol{\theta}$ to the j^{th} joint position \mathbf{p}_j in the workspace.

Consequently, the optimisation problem to be solved in this system is formulated as follows:

$$\begin{aligned} & \text{minimise } J \\ & \text{subject to } \dot{\mathbf{q}} = f(\mathbf{q}, \mathbf{u}) \\ & \mathbf{q}(t) = \mathbf{q}_{cur} \end{aligned}$$

where f is a nonlinear dynamics of the robot, \mathbf{u} is a input vector for the robot and $\mathbf{q}(t)$ is the initial state of the trajectory and corresponds to the robot's current state \mathbf{q}_{cur} . This formulation means that the calculated trajectory of the robot is limited by its dynamics and initial state.

By solving this optimisation problem with two equality constraints, we calculate the optimal state of the robot at each sampling time of the sensor, that is, the optimal trajectory of the robot $(\mathbf{q}^{(t)}, \mathbf{q}^{(t+1)}, \dots, \mathbf{q}^{(t+T_o)})^T$. This optimisation problem can be solved by a method proposed in our previous study (Kanazawa et al., 2019).

3 Experiments

In this section, we evaluate the proposed motion planning scheme using PaDY as a collaborative robot system platform. PaDY is equipped with a parts tray and a tool holder on its end-effector and delivers necessary parts and a tool to the worker involved in an assembly process of a vehicle. The worker picks up the parts and/or the tool

from the parts tray and the tool holder delivered close to the worker, and attaches the parts to their appropriate positions of the vehicle's body located overhead of the worker. For more details, please refer to Kinugawa et al. (2010).

Two sets of experiments are carried out in this section. In the first set of experiments, the worker stays at a workplace with different body orientations. We demonstrate the capability of our system to deliver parts and a tool to the worker whose orientation changes in every scenario of this experiment. We compare the results of our proposed scheme with our previous control scheme without HRI constraints in Kanazawa et al. (2019).

In the second set of experiments, we perform assembly tasks for a real vehicle body and evaluate the performance of the proposed scheme. We compare the results with our previous scheme without HRI constraints. Two scenarios are considered; when the worker is always facing the robot and when the worker is facing away from the robot.

3.1 Experiment 1: motion planning for different worker orientations

In this experiment, the robot delivers parts/tool to the worker who is standing at a fixed position in the workspace. The workspace and the experimental setup for this experiment is shown in Figures 5 and 6 respectively.

Four scenarios are prepared for this experiment:

- A1 when the worker is facing the robot
- A2 when the worker is facing away from the robot
- A3 when the worker is facing left
- A4 when the worker is facing right.

The results of the scenario A1 is shown in Figure 7. This is the case where the worker is facing the collaborative robot. We can see that the similar delivery position is calculated by the proposed scheme to that of the case without HRI constraints. Figure 8 shows the results of the scenario A2, in which the worker is facing away from the robot. In this scenario, the delivery position without HRI constraints is located behind the worker's back and the worker has to turn around every time when he/she receives the parts and the tool from the robot.

The results of the scenarios A3 and A4 are shown in Figures 9 and 10 respectively. These figures show similar results to that of the scenario A2. For the case without HRI constraints, the worker needs to turn left or right to pick the parts and the tool from the robot. However, in the proposed system taking HRI constraints into account, the robot always delivers parts in front of the worker, close to his/her dominant hand (the right hand is the dominant hand for this worker). In these experiments, we can see that the worker does not need to change his/her orientation in the workspace to accomplish given tasks by using the proposed scheme.

Figure 5 Experiment workspace (see online version for colours)



Figure 6 Experimental setup for experiment 1 (see online version for colours)

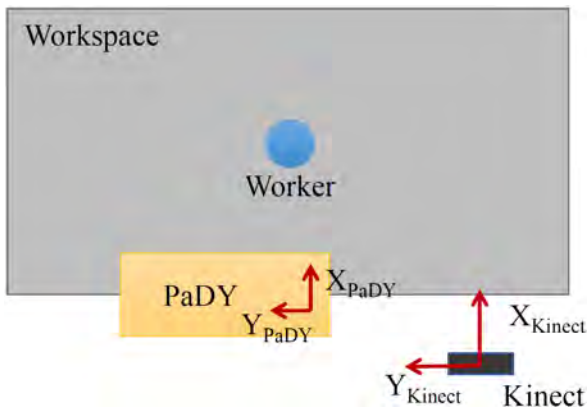


Figure 7 Scenario A1: delivery position when the worker is facing the robot, (a) previous system (b) proposed system (see online version for colours)

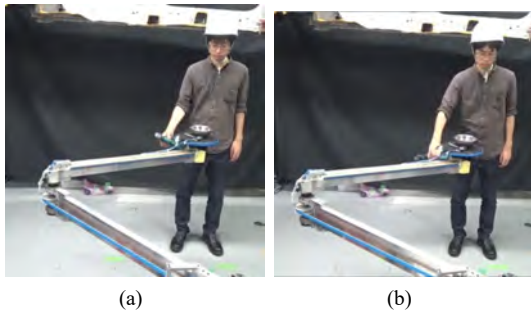


Figure 8 Scenario A2: delivery position when the worker is facing away from the robot, (a) previous system (b) proposed system (see online version for colours)

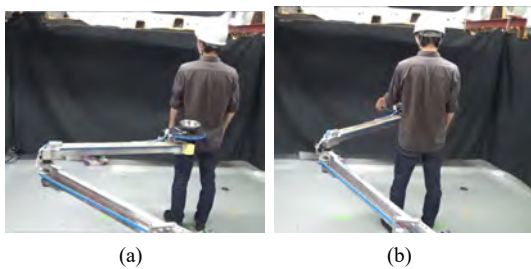
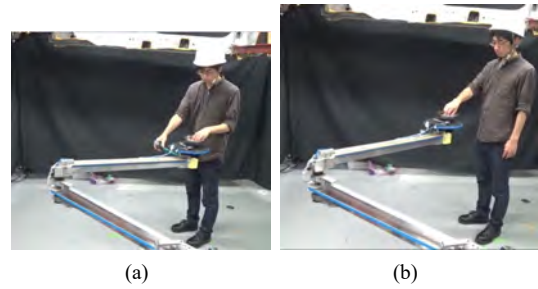


Figure 9 Scenario A3: delivery position when the worker is facing left, (a) previous system (b) proposed system (see online version for colours)



3.2 Experiment 2: motion planning for assisting automobile assembly tasks

We demonstrate the effectiveness of the proposed scheme in the following two scenarios:

- B1 the worker performs his/her tasks facing the robot
- B2 the worker performs his/her tasks facing away from the robot.

Figure 10 Scenario A4: delivery position when the worker is facing right, (a) previous system (b) proposed system (see online version for colours)



In these two experiments, the robot operates when the worker needs parts and/or a tool to complete the current task. After delivering the parts and the tool to the worker, the robot goes back to its home configuration and continues to wait there until the worker moves close to the next working position. In this experiment, we compare the results of the case without HRI constraints and the proposed scheme in two scenarios.

3.2.1 Scenario B1

The top view of the experimental setup for this scenario is shown in Figure 11. The worker performs the following tasks:

- Task 1 Attach four plug holes to the vehicle body.
- Task 2 Insert bolt(a) and tighten it using a tool.

Figure 11 Experimental setup for scenario B1 (see online version for colours)

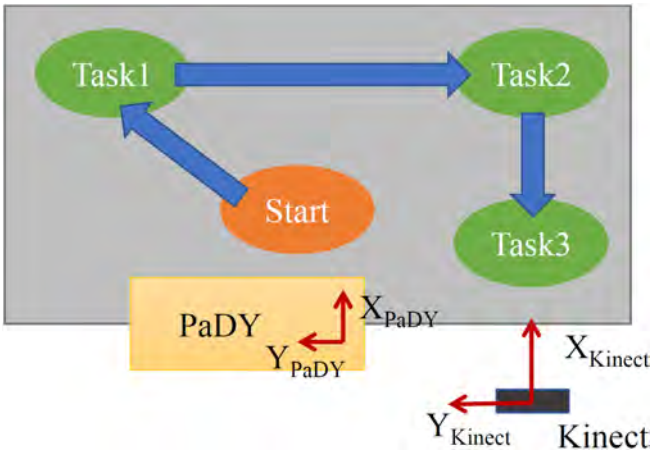


Figure 12 Using the scheme without HRI constraints in scenario B1 (see online version for colours)

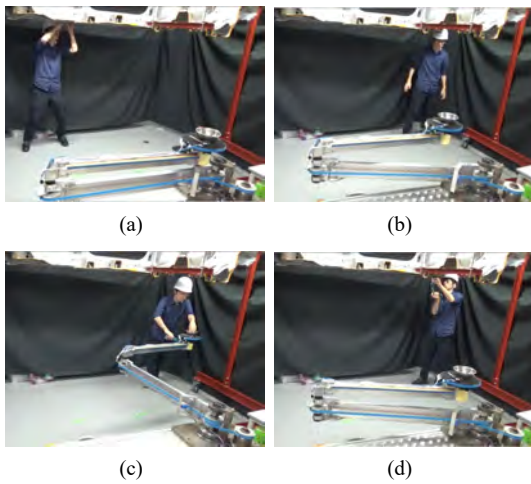
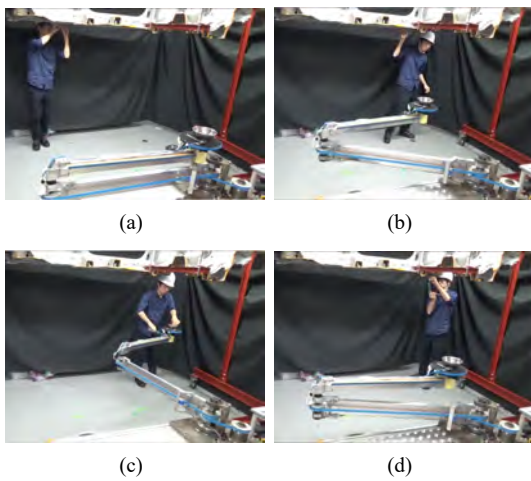


Figure 13 Using the proposed scheme in scenario B1 (see online version for colours)



We have conducted this experiment for both the case without HRI constraints and the case using the proposed scheme. The results using the scheme without HRI

constraints are shown in Figure 12, and the results using the proposed system are shown in Figure 13.

Figure 14 Experimental setup for scenario B2 (see online version for colours)

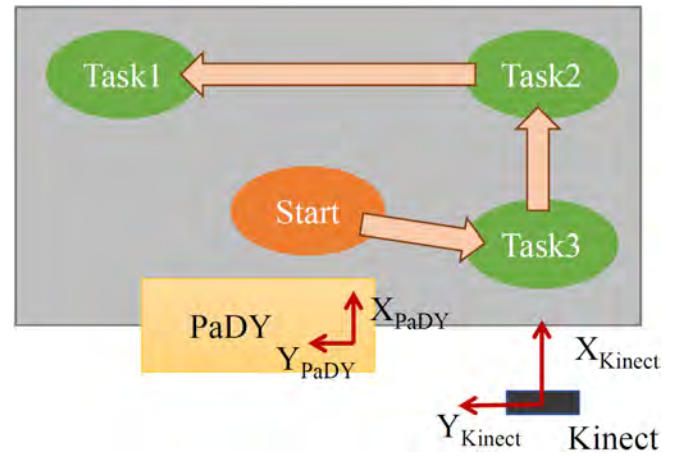
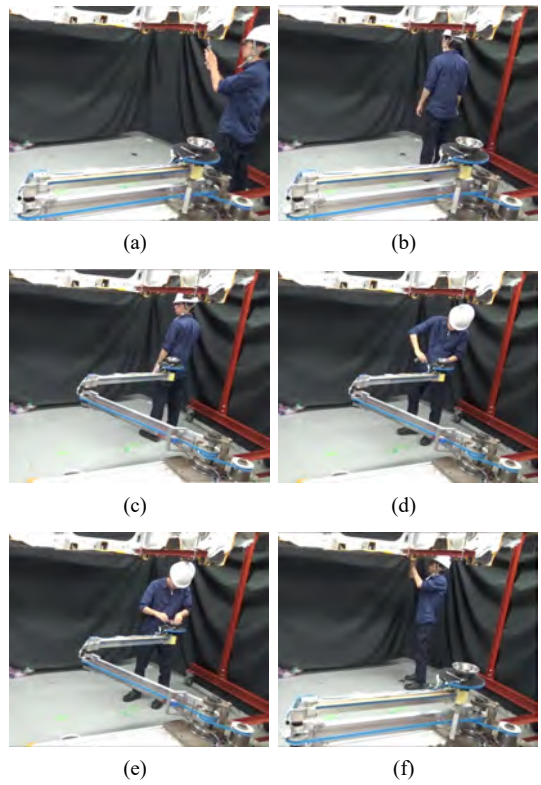


Figure 15 Using the scheme without HRI constraints in scenario B2 (see online version for colours)



This experiment is carried out as follows:

- 1 The worker performs Task 1 as shown in Figures 12(a) and 13(a).
- 2 Then the worker moves towards the location of Task 2. The robot is always observing the worker's location. When the worker's location reaches within 0.5 meter from the work position, the robot starts to move towards the worker as shown in Figures 12 and 13(b).

- 3 When the robot reaches the calculated delivery position, the worker picks up the part(s) and/or the tool from the robot's parts tray and the tool holder attached at the end of the arm as shown in Figures 12(c) and 13(c).
- 4 The worker attaches the parts to the vehicle body and accomplish Task 2. The robot returns to its home configuration and waits there until the worker needs its assistance in the following task as shown in Figures 12(d) and 13(d).

For this experiment, the results of the case without HRI constraints are similar to those of the proposed scheme with HRI constraints. This is because the worker faces the robot when he/she receives the part(s) and the tool.

3.2.2 Scenario B2

The top view of the experimental setup for this scenario is shown in Figure 14. In this experiment, the worker performs the following tasks:

- Task 2 Insert bolt(a) and tighten it using a tool.
 Task 3 Insert bolt(b) and tighten it using a tool.

We have conducted this experiment both for the case without HRI constraints and the case using the proposed scheme. The results of the case without HRI constraints and the results using the proposed scheme are shown in Figures 15 and 16 respectively.

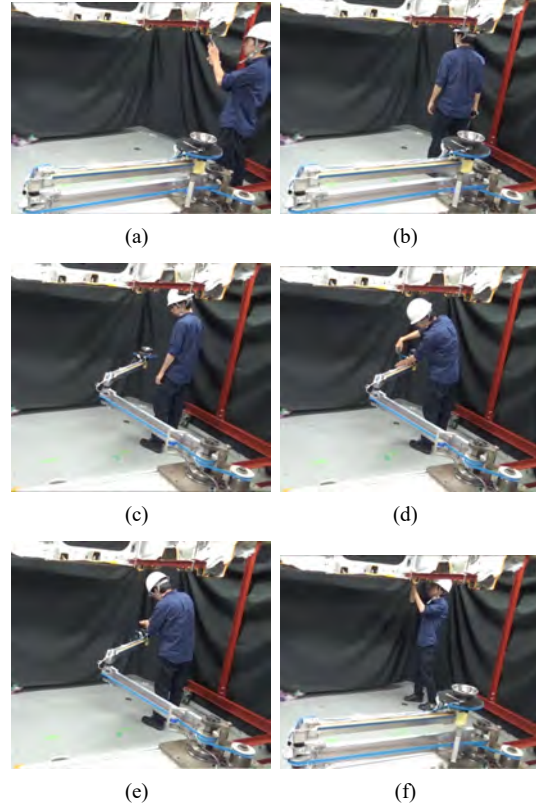
This experiment is carried out as follows:

- 1 The worker performs Task 3 as shown in Figures 15(a) and 16(a).
- 2 The worker moves towards the location of Task 2 as shown in Figures 15(b) and 16(b).
- 3 The robot is always observing the worker's location and when the worker's location reaches within 0.5 meter from the work position, the robot starts to move towards the worker as shown in Figures 15(c) and 16(c).
- 4 The worker then picks up a bolt from the parts tray and accomplish Task 2 as shown in Figures 15(e) and 16(e).
- 5 The robot returned to its home configuration where it is ready to assist the worker in the following task as shown in Figures 15(f) and 16(f).

You can see that the selection of delivery position for the robot has a profound effect on the efficiency of the worker when he/she is facing away from the robot. Without HRI constraints, the worker needs to turn around every time he/she receives the part(s) from the robot in this scenario, because the worker faces away from the robot to accomplish the Task 3 and Task 2 in this order. The proposed system always places the robot's end-effector in

front of the worker at a comfortable position for him/her with a safe distance from him. The worker can receive the part(s) and the tool from the robot quite easily in a comfortable manner.

Figure 16 Using the proposed scheme in scenario B2 (see online version for colours)



3.3 Discussion

The experimental results show that the proposed scheme with HRI constraints gives better assistance to the worker especially when the worker is not directly facing the robot. Figure 17 shows a calculated cost map in the workspace around the worker in the scenario B2. You can see that the proposed system is able to calculate the delivery position whose cost is less than that of the delivery position determined by the scheme without HRI constraints. This means that the robot flexibly adjusts its delivery position based on the worker's orientation. Since the worker's comfortable body orientation is a personal choice of the individual worker, therefore the proposed worker-centered delivery system can be applied to a collaborative work independent of the worker's preferences.

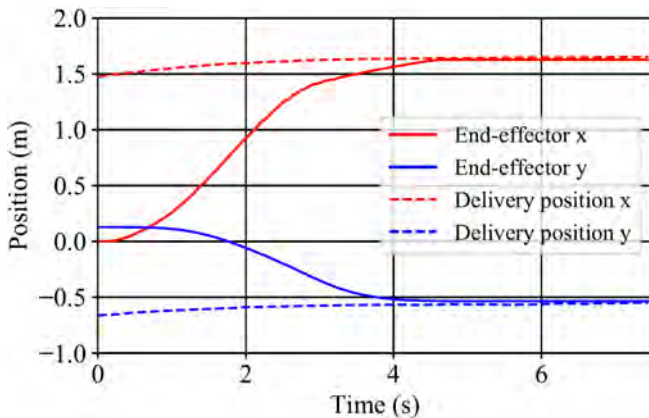
Figure 18 shows the trajectory of the calculated delivery position and robot's endpoint using proposed system in the scenario B2. Since the proposed system calculates the delivery position using the worker's body skeleton data obtained in real-time, the delivery position changes according to the changes in the position and orientation of the worker. Even if the delivery position changes, the robot's position finally converges to the delivery position

in real-time as shown in Figure 18. You can see that the proposed method plans the robot motion that converges to the appropriate delivery position in real-time as the worker approaches his/her destination.

Figure 17 Comparison of the calculated delivery positions using the proposed and previous method on the cost map in scenario B2 (see online version for colours)



Figure 18 Tracking performance of the proposed planner in scenario B2 (see online version for colours)



4 Conclusions

In this paper, we have proposed a real-time motion planning scheme that can directly plan the robot trajectory to reach the feasible and optimal delivery position calculated using HRI-based cost function.

The proposed scheme consists of the delivery position determination system and the MPC-based trajectory planning system. The delivery position determination system quickly calculates the globally optimal delivery position from the non-convex HRI cost function by applying the random sampling-based solver in the vicinity of the worker. By treating the calculated delivery position as the terminal cost and the robot's dynamic constraints and collision avoidance as the stage cost, the proposed trajectory

planning scheme could generate the robot trajectory that converges to the dynamic delivery position in real-time.

The proposed scheme was implemented in a collaborative assembly scenario in which a planar manipulator assisted the worker's automotive assembly tasks by delivering part(s) and/or a tool to the worker. Experiments conducted on several work scenarios illustrated that the proposed scheme provides more effective support than the case without HRI constraints in terms of the efficiency of collaborative work. We believe that the proposed scheme is a significant step towards better collaboration between humans and robots.

References

- Aleotti, J., Micelli, V. and Caselli, S. (2014) 'An affordance sensitive system for robot to human object handover', *International Journal of Social Robotics*, Vol. 6, No. 4, pp.653–666.
- Andersson, O., Wzorek, M., Rudol, P. and Doherty, P. (2016) 'Model-predictive control with stochastic collision avoidance using bayesian policy optimization', in *Proceedings of International Conference on Robotics and Automation (ICRA)*, pp.4597–4604.
- Cakmak, M., Srinivasa, S.S., Lee, M.K., Forlizzi, J. and Kiesler, S. (2011) 'Human preferences for robot-human hand-over configurations', in *Proceedings of IEEE/RSJ International Conference on Intelligent Robots and Systems (IROS)*, pp.1986–1993.
- Calinon, S., Bruno, D. and Caldwell, D.G. (2014) 'A task-parameterized probabilistic model with minimal intervention control', in *Proceedings of International Conference on Robotics and Automation (ICRA)*, pp.3339–3344.
- Du Toit, N.E. and Burdick, J.W. (2012) 'Robot motion planning in dynamic, uncertain environments', *IEEE Transactions on Robotics*, Vol. 28, No. 1, pp.101–115.
- Hernández, J.R., Lee, D. and Hirche, S. (2012) 'Risk-sensitive optimal feedback control for haptic assistance', in *Proceedings of International Conference on Robotics and Automation (ICRA)*, pp.1025–1031.
- ISO 10218-1:2011 (2011) *Robots and Robotic Devices – Safety Requirements for Industrial Robots – Part 1: Robots*, ISO.
- ISO 10218-2:2011 (2011) *Robots and Robotic Devices – Safety Requirements for Industrial Robots – Part 2: Robot Systems and Integration*, ISO.
- Jaillet, L., Cortés, J. and Siméon, T. (2008) 'Transition-based RRT for path planning in continuous cost spaces', in *Proceedings of IEEE/RSJ International Conference on Intelligent Robots and Systems (IROS)*, pp.2145–2150.
- Kanazawa, A., Kinugawa, J. and Kosuge, K. (2019) 'Adaptive motion planning for a collaborative robot based on prediction uncertainty to enhance human safety and work efficiency', *IEEE Transactions on Robotics*, Vol. 35, No. 4, pp.817–832.
- Kashi, B., Rosen, J., Brand, M. and Avrahami, I. (2012) 'A BiCriterion model for human arm posture prediction', in *Proceedings of World Conference on Medical Physics and Biomedical Engineering*, pp.1–4.
- Khatib, O. (1985) 'Real-time obstacle avoidance for manipulators and mobile robots', in *Proceedings of IEEE International Conference on Robotics and Automation (ICRA)*, Vol. 2, pp.500–505.

- Kim, J.J. and Lee, J.J. (2015) 'Trajectory optimization with particle swarm optimization for manipulator motion planning', *IEEE Transactions on Industrial Informatics*, Vol. 11, No. 3, pp.620–631.
- Kinugawa, J., Kawaai, Y., Sugahara, Y. and Kosuge, K. (2010) 'PaDY: humanfriendly/cooperative working support robot for production site', in *Proceedings of IEEE International Conference on Intelligent Robots and Systems (IROS)*, pp.5472–5479.
- Li, S. and Shah, J.A. (2019) 'Safe and efficient high dimensional motion planning in space-time with time parameterized prediction', in *Proceedings of International Conference on Robotics and Automation (ICRA)*, pp.5012–5018.
- Mainprice, J., Sisbot, E.A., Jaillet, L., Cortés, J., Alami, R. and Siméon, T. (2011) 'Planning human-aware motions using a sampling-based costmap planner', in *Proceedings of IEEE International Conference on Robotics and Automation (ICRA)*, pp.5012–5017.
- Ratliff, N., Zucker, M., Bagnell, J.A. and Srinivasa, S. (2019) 'CHOMP: gradient optimization techniques for efficient motion planning', in *Proceedings of International Conference on Robotics and Automation (ICRA)*, pp.489–494.
- Schulman, J., Ho, J., Lee, A.X., Awwal, I., Bradlow, H. and Abbeel, P. (2013) 'Finding locally optimal, collision-free trajectories with sequential convex optimization', in *Robotics: Science and Systems*, Vol. 9, No. 1, pp.1–10.
- Sisbot, E., Marin, L., Alami, R. and Simeon, T. (2007a) 'A human aware mobile robot motion planner', *IEEE Transactions on Robotics*, Vol. 23, No. 5, pp.874–883.
- Sisbot, E., Marin, L. and Alami, R. (2007b) 'Spatial reasoning for human robot interaction', in *Proceedings of IEEE/RSJ International Conference on Intelligent Robots and Systems (IROS)*, pp.2281–2287.
- Tanaka, Y., Kinugawa, J. and Kosuge, K. (2012) 'Motion planning with worker's trajectory prediction for assembly task partner robot', in *Proceedings of IEEE International Conference on Intelligent Robots and Systems (IROS)*, pp.1525–1532.
- Toniatti, G., Schiavi, R. and Bicchi, A. (2005) 'Design and control of a variable stiffness actuator for safe and fast physical human/robot interaction', in *Proceedings of International Conference on Robotics and Automation (ICRA)*, pp.526–531.
- Vahrenkamp, N., Arnst, H., Wächter, M., Schiebener, D., Sotiropoulos, P., Kowalik, M. and Asfour, T. (2016) 'Workspace analysis for planning human-robot interaction tasks', in *Proceedings of IEEE-RAS 16th International Conference on Humanoid Robots (Humanoids)*, pp.1298–1303.
- Wei, K. and Ren, B. (2018) 'A method on dynamic path planning for robotic manipulator autonomous obstacle avoidance based on an improved RRT algorithm', *Sensors*, Vol. 18, No. 2, pp.571–585.